2-(mix)

NASA TECHNICAL TRANSLATION NASA TT F 15, 769

REFLECTION AND REPROCESSING OF THE RADIATION OF AN X-RAY SOURCE BY THE ATMOSPHERE OF A NORMAL STAR IN A BINARY SYSTEM

M. M. Basko, R. A. Syunyayev, and L. G. Titarchuk

Translation of "Otrazheniye i pererabotka izlucheniya rentgenovskogo istochnika atmosfernoy normal'noy zvezdy v dvoynoy sisteme," Institute of Space Research of the USSR Academy of Sciences, Preprint-146, Moscow, 1974, 41 pages.

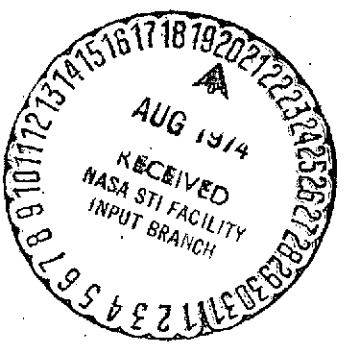

NATIONAL AERONAUTICS AND SPACE ADMINISTRATION
WASHINGTON, D. C. 20546 JULY 1974

STANDARD TITLE PAGE

1. Report No. NASA TT F 15,769	2. Government Accession No.	3. Recipient's Catalog No.
4. Title and Subtitle: Reflection and Reprocessing of the Radiation of an X-Ray Source by the Atmosphere of a Normal Star in a Binary System		5. Report Date: July 26, 1974 6. Performing Organization Code
7. Author(s): M. M. Basko, R. A. Syunyayev, L. G. Titarchuk		8. Performing Organization Report No. 10. Work Unit No.
9. Performing Organization Name and Address: SCITRAN, Box 5456, Santa Barbara, CA 93108		11. Contract or Grant No. NASw-2483 13. Type of Report and Period Covered: Translation
12. Sponsoring Agency Name and Address: National Aeronautics and Space Administration, Washington, D.C. 20546		14. Sponsoring Agency Code

15. Supplementary Notes

Translation of "Otrazheniye i pererabotka izlucheniya rentgenovskogo istochnika atmosfernoy normal'noy zvezdy v dvoynoy sisteme," Institute of Space Research of the USSR Academy of Sciences, Preprint-146, Moscow, 1974.

16. Abstract

In a closed binary system, up to 30% of the radiation of the x-ray source incident on the normal star surface is reflected by it. The remaining 70% is absorbed, being reprocessed into optical and ultraviolet radiation. The transfer of x-ray radiation is numerically investigated in the present article in a plane-parallel semi-infinite atmosphere irradiated by an externally incident flux of hard x-ray quanta. Photo absorption and Comptom scattering processes are taken into account. The values of the albedo and the spectral, polarization, spatial, and temporal (in the case of pulse primary radiation) characteristics of the reflected signal are found.

The results obtained are discussed in connection with the specific systems Her X1 and Cyg X3. The possibility of the existence of sources weak in the $h\nu \sim 2 - 6$ keV region and bright in the $h\nu \sim 15 - 20$ keV region is pointed out. The source Her X1 may be just such a source during the 24 days out of 36 when the pulsar rays are not incident on the Earth and it is possible to receive only the radiation reflected by the surface of HZ Her.

It is pointed out that the reprocessing of soft x-ray radiation in the atmosphere of HZ Her cannot explain the optical characteristics of the system. Their explanation requires hard x-ray radiation. The nature of the pulsations of the optical radiation of HZ Her is discussed.

17. Key Words (Selected by Author(s))	18. Distribution Statement: Unclassified - Unlimited		
19. Security Classif. (of this report): Unclassified	20. Security Classif. (of this page): Unclassified	21. No. of Pages: 42	22. Price

REFLECTION AND REPROCESSING OF THE RADIATION OF AN X-RAY SOURCE BY THE ATMOSPHERE OF A NORMAL STAR IN A BINARY SYSTEM

M. M. Basko,* R. A. Syunyayev,* and L. G. Titarchuk**

I. Introduction

Many of the compact galactic x-ray sources are members of /3*** binary systems whose secondary component is a normal optical star [1, 2]. In a closed system, a significant part of the radiation of the x-ray source is incident on the optical star surface. As a result, the observed optical phenomena of such systems are caused to a significant extent by the reprocessing of the x-ray radiation into optical radiation in the atmosphere of the normal component [3 — 6]. This problem and the associated problem of the necessary outflow of matter from the star surface have recently been intensively discussed in the literature [7 — 9].

X-ray radiation is absorbed upon the photoionization of hydrogen, helium, and the K-electrons in the atoms of the heavy elements. This process is effective for low energy x-ray quanta: its cross section rapidly drops as the frequency increases, $\sigma_{ph}(\nu) \sim \nu^{-3}$. Under the normal space environment of a weakly ionized plasma, the Thomson scattering cross section $\sigma_T = 6.65 \cdot 10^{-25}$ cm^2 exceeds

*Institute of Applied Mathematics, USSR Academy of Sciences.

**Institute of Space Research, USSR Academy of Sciences.

***Numbers in the margin indicate the pagination of the original foreign text.

the photoionization cross section calculated for the hydrogen atom already for photons with $h\nu_0 = 8$ keV [10, 11].

The degree of ionization of hydrogen, which appears to be the main supplier of electrons, has practically no effect on the photoabsorption cross section (the main contribution to the total absorption cross section of quanta with $h\nu > 1$ keV is that of the heavy elements) nor on the cross section for x-ray quanta scattering. At $h\nu > \alpha M_e c^2 \approx 3.7$ keV, when the wavelength of a quantum is less than the Bohr orbit radius, the scattering of hard x-ray radiation by hydrogen and helium atoms is accompanied by the removal of an electron, since the recoil energy $\sim h\nu(h\nu/M_e c^2)$ exceeds hydrogen ionization potential $\left[I_H = \frac{1}{2}\alpha^2 M_e c^2\right]$. Thereupon, the cross section for scattering by electrons associated with the hydrogen atoms does not differ from the scattering cross section of free electrons. Here $\left[\alpha = \frac{2\pi e^2}{hc} = \frac{1}{137}\right]$ is the fine structure constant.

At the same time, a high degree of ionization of helium and /4 the heavy elements C, N, O, Ne, and so on, results in a decrease in the total absorption cross section and shifts the point at which $\left[\overline{\sigma_{ph}(\nu)} \approx \sigma_T\right]$ in the direction of lower energy quanta $h\nu < 8$ keV.

Thus, the fate of x-ray photons incident on the photosphere of a normal star depends on their initial energy: in the case of $h\nu \lesssim 8$ keV, they are absorbed and their energy is reprocessed into the energy of soft (and, in particular, optical) radiation; in the case where $h\nu \gg 8$ keV, a significant part (already 17% in the case of single scattering) of the incident photons is reflected [7].

A number of compact x-ray sources and, in particular, both x-ray pulsars, which are components of double star systems — Her X1 and Cen X3-possess an anomalously hard radiation spectrum $kT_x \sim 30$ keV [12]. Therefore, the problem of explaining the fraction of the reflected energy, namely, the albedo of the normal component in the hard x-ray region, is of particular interest. In the first place, we are interested from the point of view of the efficiency of the reprocessing of hard x-ray radiation into optical radiation in the atmosphere of the normal component of the binary system. And in the second place, the characteristics of the reflected signal itself, especially in the case in which the primary directional radiation is not incident on the Earth, are of interest.

We note that the absorption of the energy of hard x-ray radiation is associated both with photoionization accompanied by the photon destruction and also with the recoil effect in the case of scattering $\left[\frac{\Delta\nu}{\nu} \sim -\frac{h\nu}{m_e c^2}\right]$. The recoil effect plays a dual role here: on the one hand, at each scattering, a part of the photon energy is transmitted to the electron, and after a number of scatterings $\left[\sim \frac{m_e c^2}{h\nu}\right]$, a photon loses a significant part of its energy; on the other hand, a decrease in the photon energy due to recoil increases the probability of its photoabsorption, which also leads to a decrease in the albedo. For energetic quanta, the recoil effect plays a fundamental role in energy absorption. Thus, for example, the two-dimensional albedo amounts to 47% for a monochromatic line with $h\nu = 30$ keV. /5 Numerical calculations carried out with the neglect of photoabsorption ($\sigma_{ph} = 0$) have resulted in an albedo equal to 65% (see Table I), i.e., the absorption of energy has decreased by only one-third.

TABLE I*

Monochromatic line hν (keV)	Two-dimensional energy albedo A_p		Two-dimensional albedo based on number of quanta A_{pn}		Two-dimensional energy albedo A_p for $\sigma_{ph}=0$	Spherical energy albedo	Mean number of scatterings $\bar{N}$
	$\mu_0=1$	$\mu_0=0,5$	$\mu_0=1$	$\mu_0=0,5$	$\mu_0=1$		$\mu_0=1$
15	0,24	0,33	0,27	0,36	0,75	-	6,7
30	0,47	0,6	0,6	0,73	0,65	-	30
60	0,45	0,6	0,7	0,8	0,5	-	45
Continuous spectrum with kT_x (keV)							
15	0,21	0,26	-	-	0,73	0,24	-
30	0,30	0,39	-	-	0,66	0,36	-

*[Translator's Note: Commas in numbers indicate decimal points.]

In the third part of this article, values of the two-dimensional and spherical albedo (Table I) are derived by means of a numerical solution of the transfer equations for x-ray radiation in a plane-parallel atmosphere (worked out in the second part and taking account of scattering and photo-absorption processes). The problem of short-period pulses of reflected x-ray radiation (Section IV, d) and optical radiation arising from the reprocessing as absorbed x-ray flux (IV, e), is investigated.

The fifth part is devoted to astrophysical applications. The fraction of the energy of the x-ray flux from the source Her X1 which has been reprocessed into optical radiation of the visible component of the system HZ Her is estimated. It is shown that soft x-ray radiation with $h\nu < 1$ keV, which has been assumed in a number of papers [13, 8] to explain the optical variability of HZ Her, cannot give the observed optical characteristics of HZ Her. Only the reprocessing of the hard x-ray radiation of Her X1 can give the properties.

Up to 30% of the hard ($h\nu \sim 15$ — 30 keV) x-ray radiation incident on the surface of HZ Her should be reflected by it. As a result, the hard x-ray radiation of the system Her X1 = HZ Her should be observed on Earth (at a level ~ 10% of the maximum flux) and during those 24 days of the 36 in which the strongly directional soft ($h\nu < 10$ keV) x-ray radiation is not incident on the Earth (see Section V, a). This effect — the reflection of hard x-ray radiation by the surface of the normal component — opens up the possibility of a search for x-ray pulsars into whose directional diagram the Earth does not fall.*

*In the opposite case, the reflection effects cause an insignificant oscillation in the primary x-ray brightness curve.

The x-ray brightness curve of such binary systems is shown in Figure 1. It is similar to that observed for the x-ray source Cyg X3 in the case of an orbital inclination of i ~ 10° — 15° (see Section 5b). /6

The spectrum of the reflected x-ray radiation is shown in Figure 2. It has a characteristic maximum at $h\nu \sim 15$ — 20 keV. A result of this is the possibility of the existence of a population of x-ray sources which appear only in the hard x-ray region and are practically unobservable in the standard region of $h\nu \sim 2$ — 6 keV. On the other hand, as has been shown in Section 4b, under certain conditions the surface of the normal star can effectively reflect x-ray radiation in the $h\nu \sim 3$ — 10 keV region. Discontinuities should appear in the spectrum of the reflected radiation corresponding to the boundaries of the K-series absorption of atoms of the heavy elements Fe, S, and Ar. The most important distinctive feature of the spectrum is a strong emission of the K_α-line of iron. The reflected radiation is characterized by its noticeable linear polarization (the natural consequence of Thomson scattering) whose degree depends on the observation phase and the orbital inclination i.

II. Equations of Transfer in a Plane-Parallel Atmosphere

a. Statement of the Problem

The absorption and scattering of hard x-ray radiation $h\nu \gtrsim 10$ keV incident on the surface of the normal component takes place primarily in the photospheric layers (see the results of the calculations in [7]), where $T_e \lesssim 2 \cdot 10^{40}$ K. This allows:

1. the star atmosphere to be assumed plane-parallel at each point, since the thickness of an exponential atmosphere $H \approx \frac{kT_e R^2}{m_p G M} \ll R$ — the star radius;

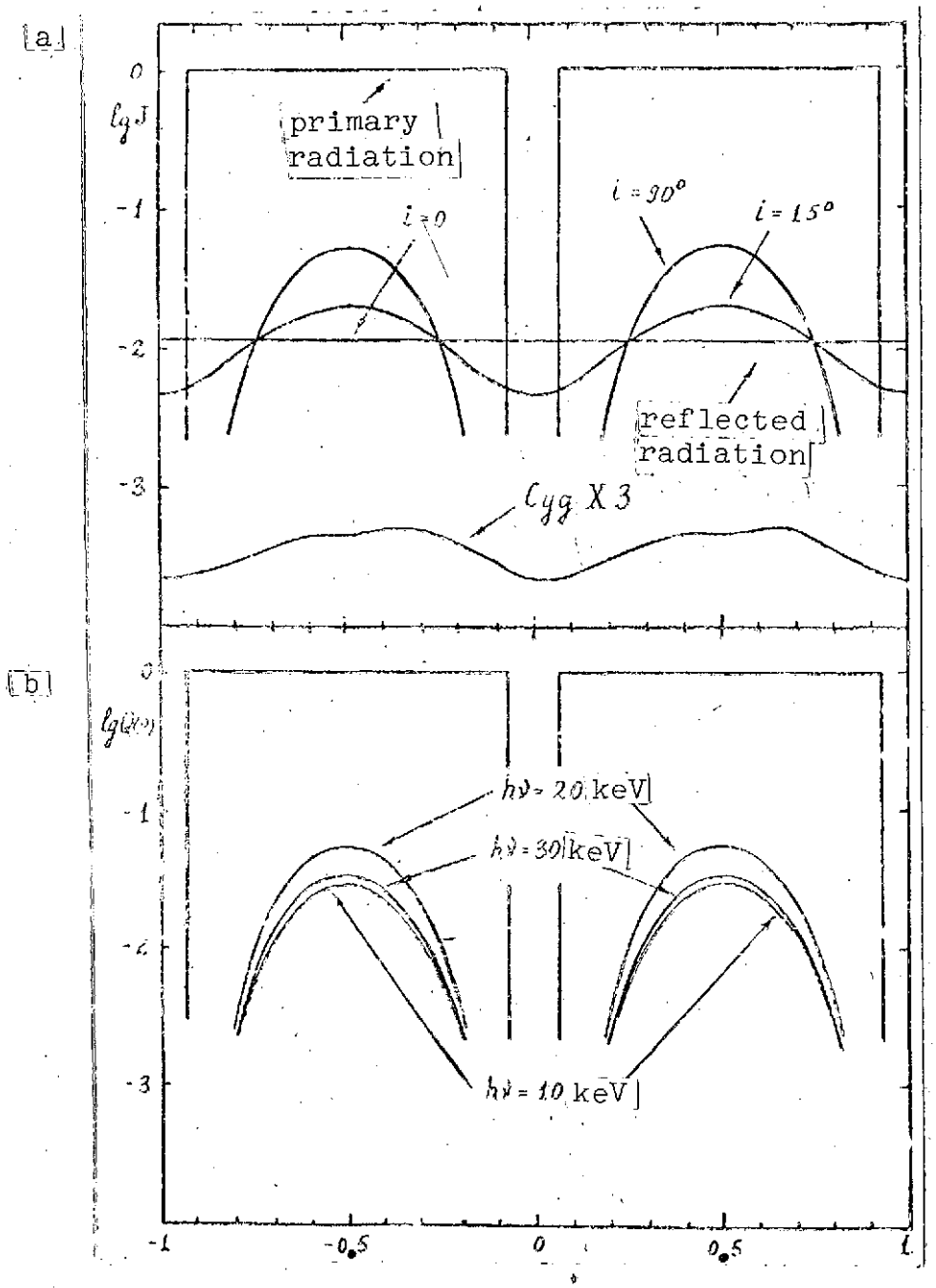

Figure 1. Integrated (for different orbital inclinations i) and spectral curves of the x-ray brightness of the HZ Her system in reflected light. The temperature of the primary x-ray radiation is kT_x = 30 keV. The mean observed curve of the x-ray brightness of the source Cyg X3 is shown for comparison in Figure 1a as a function of the phase of the 4.8-hour cycle.[28].

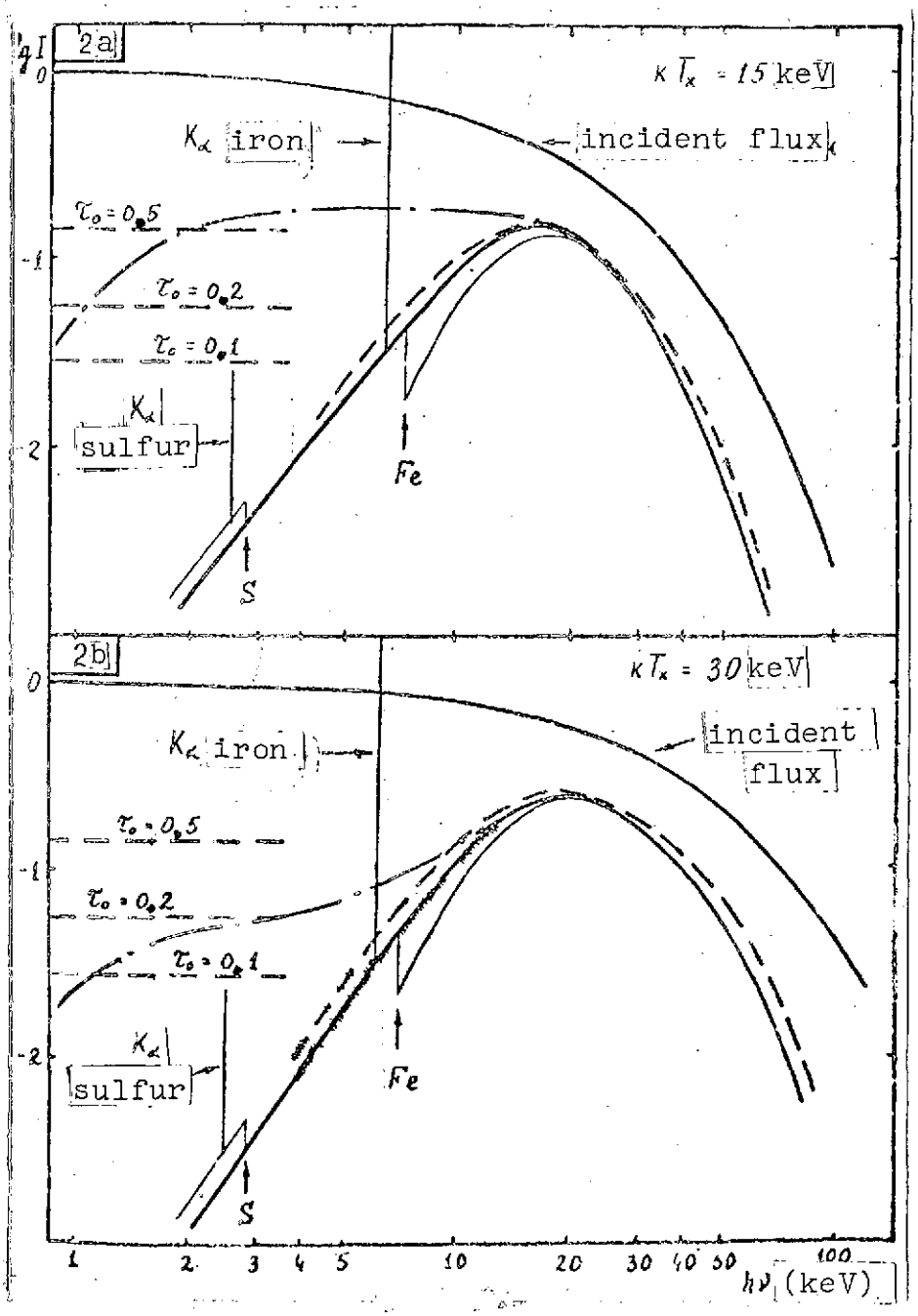

Figure 2. Spectrum of the x-ray radiation reflected from a semi-infinite plane-parallel atmosphere. The primary flux with a spectral dependence of the form (23) with kT_x = 15 and 30 keV is incident along the normal to the surface. The solid line depicts the spectrum of the radiation reflected normally to the atmosphere surface, and the dashed line indicates that reflected at an angle of 90° to the normal. The horizontal dashed lines correspond to a signal reflected from the external high temperature scattering layer of different optical [Continued on page 9]

[Figure 2, continued] thickness for Thomson scattering τ_0. The dot-dashed line depicts an example spectrum of the reflected radiation when such a layer is present. The normalization of the curve is explained in section III. Details of the spectrum are taken into consideration in the curve shown as a thin line.

2. the complete neglect of ionization of K-electrons of the heavy elements and the use of the results of the calculation cited in [14, 11] for the photoabsorption cross section; and

3. the electrons to be considered at rest for Compton scattering of x-ray quanta, since $\kappa T_e \ll h\nu(h\nu/m_e c^2)$.

X-ray radiation in the 2 keV $\leq h\nu \leq$ 50 keV, in which one can assume with sufficient accuracy that $x = \frac{h\nu}{m_e c^2} \ll 1$, the scattering cross section to be the Thomson cross section, and the scattering indicatrix to be isotropic, is of practical interest in the problem being discussed. /7

Below are given the basic equations on the basis of which the numerical calculations were carried out. We will introduce a system of coordinates OXYZ, whose OZ axis is pointed in the direction of decreasing density perpendicular to the star surface. A flux of external radiation $H(\nu)$ (ergs/cm^2 sec Hz) is incident on the atmosphere in the OXZ plane at an angle of $\vartheta_0 = \arccos\mu_0$ to the OZ axis. As independent variables, we will use in what follows the optical thickness for Thomson scattering $\tau = \sigma_T \int_z^\infty N_e(z)dz$, the azimuthal angle φ (measured in the OXY plane from the OX axis), and $\mu = \cos\vartheta$ (where ϑ is the polar angle measured from the OZ axis). We adopt for the photoabsorption cross section of x-ray quanta of frequency ν

$$\sigma(\nu) = \sigma_T + \sigma_{ph}(\nu) = \sigma_T[1 + (\nu_0/\nu)^3], \quad (1)$$

where $h\nu_0$ = 8 keV. The chemical environment is assumed to be normal. Then the probability of the "survival" of a quantum at

each absorption event is

$$\lambda(\nu) = \sigma_T/\sigma(\nu) = [1+(\nu_0/\nu)^3]^{-1}. \qquad (2)$$

b. Equation of Transfer

The equation of transfer of x-ray radiation in the approximation of isotropic scattering by electrons at rest, taking into account photoabsorption and the recoil effect, has the form:

$$\mu \frac{\partial I(\nu,\tau,\mu,\varphi)}{\partial \tau} = \lambda^{-1}(\nu) I(\nu,\tau,\mu,\varphi) - \frac{1}{4\pi}\int_0^{2\pi} d\varphi' \int_{-1}^{1} \frac{\nu}{\nu'}\frac{\partial \nu'}{\partial \nu} I(\nu',\tau,\mu',\varphi') d\mu' - \frac{1}{4\pi}\frac{\nu}{\nu_1'}\frac{\partial \nu_1'}{\partial \nu} H(\nu_1') \exp[-\tau\mu_0^{-1}\lambda^{-1}(\nu_1')], \qquad (3)$$

where $I(\nu,\tau,\mu,\varphi)$ is the intensity of the x-ray radiation, and

$$\nu' = \nu/[1-(h\nu/m_e c^2)(1-\cos\gamma)]; \qquad (4)$$

$$\cos\gamma = \mu\mu' + \sqrt{(1-\mu^2)(1-\mu'^2)}\cos(\varphi-\varphi'); \qquad (5)$$

$$\nu_1' = \nu/[1-(h\nu/m_e c^2)(1+\cos\gamma_0)]; \qquad (6)$$

$$\cos\gamma_0 = \mu\mu_0 + \sqrt{(1-\mu^2)(1-\mu_0^2)}\cos\varphi. \qquad (7)$$

We note that it follows from Equations (4) and (6) that /8
$\frac{\partial \nu'}{\partial \nu} = \left(\frac{\nu'}{\nu}\right)^2$ and $\frac{\partial \nu_1'}{\partial \nu} = \left(\frac{\nu_1'}{\nu}\right)^2$. Introducing the source function

$$S(\nu,\tau,\mu,\varphi) = \frac{1}{4\pi}\int_0^{2\pi} d\varphi' \int_{-1}^{1} \frac{\nu'}{\nu} I(\nu',\tau,\mu',\varphi') d\mu' + \frac{1}{4\pi}\frac{\nu_1'}{\nu} H(\nu_1') \exp[-\tau\mu_0^{-1}\lambda(\nu_1')] \qquad (8)$$

and solving Equation (3) with the boundary condition $I(\nu,0,\mu,\varphi)\big|_{\mu<0} = 0$ we derive an integral equation for $S(\nu,\tau,\mu,\varphi)$

$$S(\nu,\tau,\mu,\varphi) - \frac{1}{4\pi}\int_0^{2\pi} d\varphi' \left\{ \int_{-1}^{0} \frac{\nu'}{\nu}\frac{d\mu'}{\mu'} \int_0^{\tau} \exp[(\tau-\xi)\mu^{-1}\lambda^{-1}(\nu')]\, S(\nu',\xi,\mu',\varphi') d\xi + \right.$$
$$\left. + \int_0^{1} \frac{\nu'}{\nu}\frac{d\mu'}{\mu'} \int_{\tau}^{\infty} \exp[(\tau-\xi)\mu^{-1}\lambda^{-1}(\nu')] S(\nu',\xi,\mu',\varphi') d\xi \right\} = \frac{1}{4\pi}\frac{\nu_1'}{\nu} H(\nu_1') \exp[-\tau\mu_0^{-1}\lambda^{-1}(\nu_1')].$$

c. Assumed Approximation

In the frequency region of interest to us, one can, with sufficient accuracy, assume $x = h\nu/m_e c^2 \ll 1$. It is evident from Equation (9) that $S(\nu,\tau,\mu,\varphi)$ depends on φ and μ only through ν' and ν_1'. If the right-hand side of this equation changes weakly in the frequency interval $\Delta\nu = \nu\frac{h\nu}{m_e c^2} = \frac{m_e c^2}{h}x^2$, which corresponds to an average frequency shift of a quantum in the case of single scattering, that is, in the case where

$$\frac{\Delta H}{H} = \frac{1}{H}\frac{\partial H}{\partial x}x^2 \ll 1, \tag{10}$$

then the source function $S(\nu,\tau,\mu,\varphi)$ also depends weakly on μ and φ by virtue of the continuous dependence of the solution of the integral equation (9) on the right-hand side. This permits the use in finding the intensity $I(\nu,\tau,\mu)$ with sufficient accuracy of source functions averaged over the angles $S_1(\nu,\tau,\mu) = \frac{1}{2\pi}\int_0^{2\pi} S(\nu,\tau,\mu,\varphi)d\varphi$ and $S_2(\nu,\tau) = \frac{1}{2}\int_{-1}^{1} S_1(\nu,\tau,\mu)d\mu$, equations for which to an accuracy of terms of the second order in x are derived from Equation (9) by the substitution $\nu' = \nu/[1-x(1-\mu\mu')]$ for S_3 (approximation III) and by the substitution of $\nu' = \nu/(1-x)$ for S_2 (approximation II). In the numerical calculations, approximation II was used as the main one, the integral equation for which has the form

$$S_2(x,\tau) = \frac{3}{(1-x)^3}\left[\frac{1}{2}\int_0^{\infty} E_1(|\tau - t/\lambda(\tfrac{x}{1-x})|)\, S_2(\tfrac{x}{1-x},t)dt + \frac{1}{4\pi}\frac{1}{(1-x)^2}H(\tfrac{x}{1-x})\exp[-\tau\mu_0^{-1}\lambda^{-1}(\tfrac{x}{1-x})]\right], \tag{11}$$

where $E_n(x) = \int_1^{\infty} e^{-x\xi}\xi^{-n}d\xi$ is the integral exponential function of order n. Approximation I (the crudest one) differs from approximation II in that in Equation (11), the value of $S_2(x,\xi)$ at $\xi = \tau$ is removed from under the integral. We note that $E_1(x) = -\ln x + O(x)$ at $x \to 0$, and $\int_0^{\infty} E_1(x)dx = 1$.

/9

Thus, in approximation I, we have

$$S_1(x,\tau)=\frac{1}{1-x}\lambda\left(\frac{x}{1-x}\right)\left[1-\frac{1}{2}E_2\left(\tau/\lambda\left(\frac{x}{1-x}\right)\right)\right]S_1\left(\frac{x}{1-x},\tau\right)+$$
$$+\frac{1}{4\pi}\frac{1}{1-x}H\left(\frac{x}{1-x}\right)\exp\left[-\tau\mu_0^{-1}\lambda^{-1}\left(\frac{x}{1-x}\right)\right]. \qquad (12)$$

Approximation III is not the next most accurate in comparison with II, as an approximation to the angular dependence, since the dependence of $S(x,\tau,\mu,\varphi)$ on φ is not so significant as its dependence on μ. However, one can assess the degree of agreement of approximation III and II by the error which we allow using approximation II.

The intensity of the reflected flux calculated according to approximation II is illustrated by a solid line and that calculated according to approximation I is illustrated by a dotted line in Figures 3 and 4, and the intensity calculated according to approximation III is illustrated by a dashed line in Figure 4. Plots are given in Figure 4 for the x-ray radiation fluxes incident and reflected from a plane-parallel atmosphere for the case of $\mu = \mu_0 = 1$, when the incident flux is concentrated in a spectral interval less than $\Delta\nu = \nu x$ near $h\nu = 30$ keV. Condition (10) is violated, and the large discrepancy in approximations III and II indicate their inapplicability for determining the intensity of the x-ray flux emergent after several former scatterings. At the same time, the values of the albedo (which is an integral characteristic of the problem) derived in these two approximations are practically identical. The presence of a narrow peak shifted by $2\Delta\nu$ in frequency is easily explained by the fact that in order for x-ray quanta to emerge, it is necessary to get "unfolded" by 180°. For spectrally wide radiation of the form (23), when the condition (10) is fulfilled with sufficient accuracy, the spectral differences between approximations III and II do not exceed 3%, which completely confirms the application of Equation (11) to the problem under discussion. We note

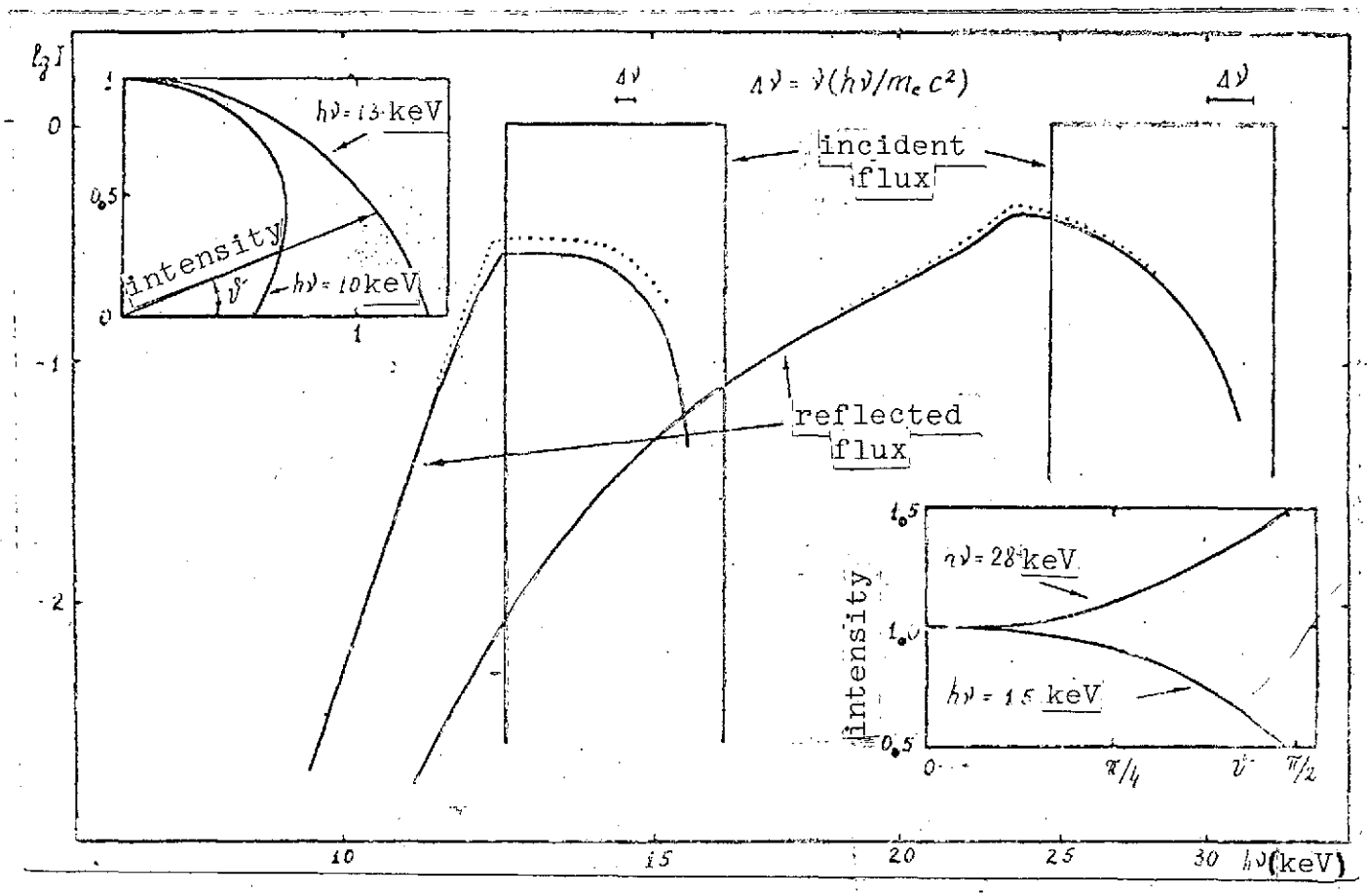

Figure 3. Spectrum of the reflected flux in the case of normal incidence on a plane-parallel atmosphere of a monochromatic line with hν = 15 and 30 keV. In the upper left-hand corner, the graph represents, in polar coordinates, the directionality of the reflected radiation for two values of the energy of reflected quanta for an incident line with hν = 30 keV. The very same quantities are illustrated in the lower right-hand corner in the usual coordinates for an incident line with hν = 30 keV.

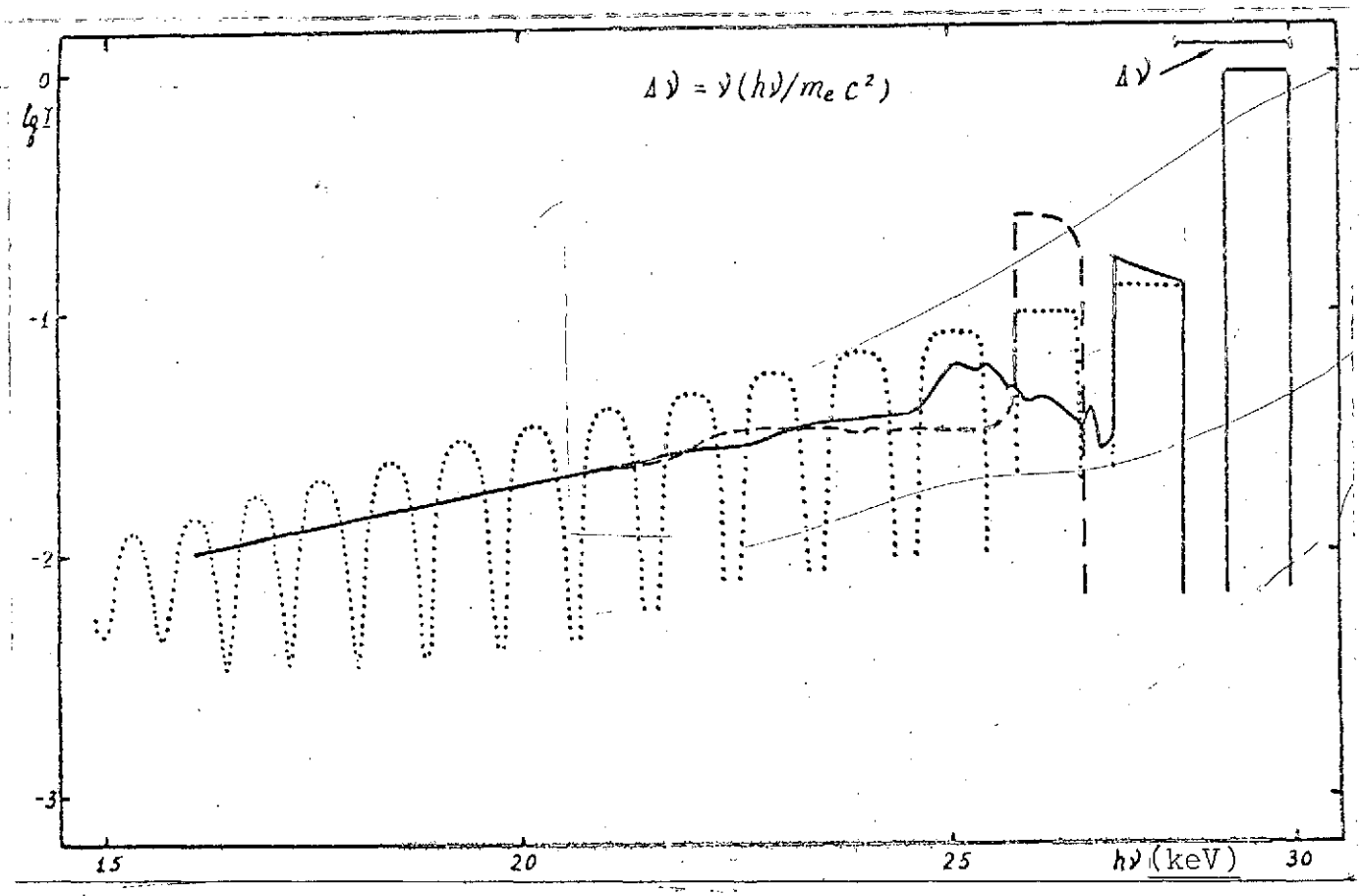

Figure 4. Spectrum of the radiation emergent normally to the surface of the atmosphere when a monochromatic line $h\nu$ = 30 keV is incident on it also along the normal to the surface. The dotted line depicts the results of calculations based on approximation I, the solid curve denotes calculations based on approximation II, and the dashed line illustrates calculations based on approximation III (see Section II).

that Equations (10) and (12) are actually not integral equations but recurrence relations. /10

The energy two-dimensional albedo A_p, the albedo based on the number of quanta A_{pn}, and the average number of scatterings of incident x-ray quanta $\bar{N}$ prior to absorption or exit from the scattering zone have been determined from the following equations:

$$A_p = \frac{2\pi}{\mu_0} \frac{\int_0^\infty dx \int_0^1 \mu I(x,0,\mu)\,d\mu}{\int_0^\infty H(x)\,dx}, \qquad (13)$$

$$A_{pn} = \frac{2\pi}{\mu_0} \frac{\int_0^\infty x^{-1} dx \int_0^1 \mu I(x,0,\mu)\,d\mu}{\int_0^\infty H(x)\,x^{-1}\,dx}, \qquad (14)$$

$$\bar{N} = \frac{4\pi}{\mu_0} \frac{\int_0^\infty x^{-1}\lambda^{-1}(x)\,dx \int_0^\infty S_2(x,\tau)\,d\tau}{\int_0^\infty H(x)\,x^{-1}\,dx}. \qquad (15)$$

The quantity $\bar{N}$ is the ratio of the total number of scatterings in a vertical column (of unit cross section) of the atmosphere to the flux of incident quanta.

d. Dependence of the Two-Dimensional Energy Albedo on the Energy of the Quanta

Let a monochromatic flux of hard quanta be normally incident on a semi-infinite atmosphere. We will discuss two different limiting cases corresponding to low and high frequencies:

1) the scattering is isotropic and monochromatic, the role of photoabsorption is significant, and the role of the recoil effects is minor: $\lambda(\nu) = [1 + (\nu_0/\nu)^3]^{-1}$; and

2) the scattering occurs by electrons at rest, the role of photoabsorption is negligibly small, $\lambda(\nu) = 1$, and the exact relativistic equations are used for the scattering cross section and the recoil effect.

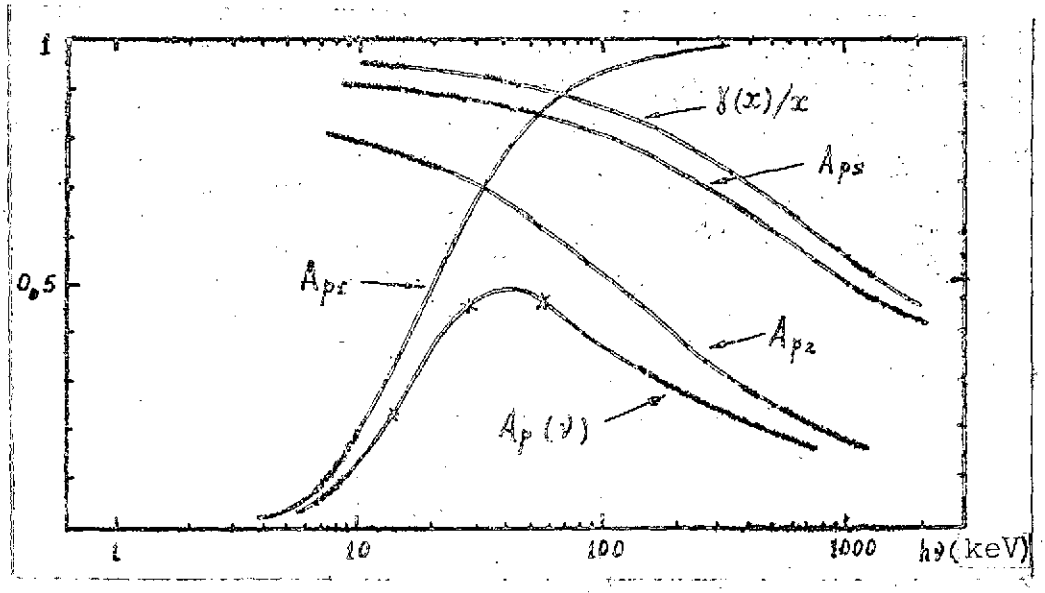

Figure 5. Dependence of the energy albedo of a plane-parallel semi-infinite atmosphere on the energy of the x-ray quanta incident along the normal to the surface.

$A_p(\nu)$- photoabsorption and the recoil effect taken into account; $A_{p1}(\nu)$- only photoabsorption taken into account; $A_{p2}(\nu)$- only the recoil effects taken into account (example form); $A_{ps}(\nu)$- upper estimate (see Section IIb) for $A_{p2}(\nu)$; $\gamma(x)$- average energy (in units of mec^2) after scattering of the quanta with the initial energy; the results of the numerical calculations are denoted by small ×.

Case 1) gives a good description of the reflection of x-ray radiation from an atmosphere with a normal chemical composition in the case of $h\nu \lesssim 8$ keV. This case has been investigated in detail [15, 16], and a plot of the corresponding albedo $A_{p1}(x)$, where $x = h\nu/m_e c^2$, is given in Figure 5. Case 2) corresponds to the reflection of high frequency radiation ($h\nu \gg 8$ keV) from a semi-infinite medium. An example form of the two-dimensional albedo $A_{p2}(x)$ in this case is also given in Figure 5. It is clear that the actual value of the albedo of a monochromatic line $A_p(x)$ should satisfy the inequalities $A_p(x) < A_{ps}(x)$ and /11 $A_p(x) < A_{p2}(x)$ (see Figure 5). It follows from this that, at a

certain frequency $x = x^*$, the quantity $A_p(x)$ reaches its maximum value $A_p^* = A_p(x^*) < 1$. Numerical calculations (see Table I) and the estimates cited below show that the energy $h\nu^* = x^* m_e c^2 \approx 50$ keV, and $A_p^* \approx 50\%$.

Estimates of $A_{p2}(x)$. The differential scattering cross section of a photon by an electron at rest [17] has the form

$$d\sigma(x,\zeta) = \frac{1}{2}\frac{e^4}{m^2c^4}\,\varphi(x,\zeta)\,d\zeta,$$

where arc cos ζ is the scattering angle and

$$\varphi(x,\zeta) = \frac{1}{[1+x(1-\zeta)]^2}\left[1+\zeta^2+\frac{x^2(1-\zeta)^2}{1+x(1-\zeta)}\right]. \qquad (16)$$

The average energy (in units of $m_e c^2$) of the photons after the first scattering is

$$\gamma(x) = \frac{\int_{-1}^{1} x\varphi(x,\zeta)\,d\zeta/[1+x(1-\zeta)]}{\int_{-1}^{1}\varphi(x,\zeta)\,d\zeta} = \frac{\omega(x)}{2\psi(x)}, \qquad (17)$$

$$\frac{1}{2}\int_{-1}^{1}\varphi(x,\zeta)\,d\zeta = \psi(x) = \left(\frac{1}{2x}-\frac{1+x}{x^3}\right)\ln(1+2x)+\frac{2}{x^2}+\frac{1+x}{(1+2x)^2}, \qquad (18)$$

$$\omega(x) = \frac{\ln(1+2x)}{x^2}+\frac{1}{3}\left[1-\frac{1}{(1+2x)^3}\right]+\frac{2x^2-2-2/x}{1+2x}. \qquad (19)$$

Since the energy of the photons upon succeeding scatterings can only decrease, then

$$A_{p2}(x) < \psi(x)/x = \frac{1}{3}(\ln x)^{-2}+O\left(\frac{1}{x}\right). \qquad (20)$$

It follows from this estimate that $A_{p2}(x) \to 0$ and $x \to \infty$ and has the form given in Figure 5. Taking the frequency shift at the second scattering into account permits deriving a more accurate estimate for the quantity $A_{p2}(x)$:

$$A_{ps}(x) < A_{ps}(x) = \frac{\varphi(x)}{2\psi(x)}\left[\frac{1}{1+x} - \frac{1}{x}\chi\left(\frac{x}{1+2x}\right) + \frac{\omega(\chi(x))}{2\psi(x)}\right], \quad (21)$$

where

$$\varphi(x) = \frac{2}{x^2} + \left(2 + \frac{1}{x} - \frac{3}{x^2} - \frac{2}{x^3}\right)\ln\frac{1+2x}{1+x} + \frac{2x^3 + \frac{9}{2}x^2 + \frac{3}{2}x + 1}{(1+2x)x^2(1+x)^2} - 2\ln 2. \quad (22)$$

A plot of the function $A_{ps}(x)$ is given in Figure 5.

III. Results of Numerical Calculations

a. Reflection from a Plane-Parallel Atmosphere

The results of numerical calculations are given in Table I and depicted in the figures. Plots are given in Figure 3 of the intensity of the fluxes of x-ray radiation incident at an angle /12 $\vartheta_0 = \arccos\mu_0 = 0$ and reflected from a plane-parallel semi-infinite atmosphere at an angle of $\vartheta = \arccos\mu = 0$, for the case in which the incident flux is concentrated in a narrow spectral interval near $h\nu_1$ = 15 keV and $h\nu_2$ = 30 keV. We note that the width of this spectral interval is restricted from below by the condition (10) of the applicability of the approximations used.

Transfer equations are linear with respect to the intensity $H(\nu)$ (dimensions of ergs/cm^2 sec Hz). The adopted normalization of the radiation intensity is such that a spectral energy flux $\pi\mu_0 H(\nu) = \pi$ is incident on a cross section of unit area. If the surface of the semi-infinite atmosphere were to reflect this entire flux without a change in frequency and isotropically in all directions, the reflected radiation would have an intensity of unity. The fraction of the reflected energy (the two-dimensional energy albedo), the fraction of the reflected number of quanta, and the average number of scatterings for an incident

flux with frequencies of $h\nu$ = 15, 30, and 60 keV are given in Table I. As the photon energy increases, the accuracy of the non-relativistic approximation drops; therefore, the actual values of the albedo for $h\nu$ = 60 keV may differ somewhat from the values cited in Table I.

As the frequency increases, the role of photoabsorption decreases, but the Compton energy losses associated with the recoil effects increase. Therefore, as the frequency increases, the monochromatic line albedo $A_p(\nu)$ for $\nu < \nu^*$ increases, reaches a maximum value $A_p^* \sim 0.5$ at $h\nu^* \sim 50$ keV, and decreases to zero for $\nu^* < \nu \to \infty$ (see Figure 5 and Section IId). Thus, due to the recoil effect in the case of Compton scatterings, no less than one-half of the energy of the x-ray flux incident normally on the surface of the optical star is absorbed and goes into heating up the atmosphere.

In the upper left-hand corner of Figure 3, a plot is given for the intensity of the emergent radiation as a function of the angle of emergence ϑ (in polar coordinates) for two values of the energy, for the case in which a monochromatic line $h\nu$ = 15 keV is incident. In the lower right-hand corner, the same plot [in the usual coordinates $I_\nu(\vartheta)$] is given for an incident line with $h\nu$ = 30 keV. We recall that an element of the surface with area dS reflects a flux of energy per unit solid angle of $dF_\nu(\vartheta) = I_\nu(\vartheta)\cos\vartheta\, dS$. The harder quanta — which have experienced one or two scatterings — emerge mainly at angles close to $\pi/2$, whereas the softer quanta, which have experienced more scatterings, emerge mainly at small angles to the normal. /13

The spectrum of the reflected radiation for the case in which an x-ray flux with a spectral dependence

$$I(\nu) = \pi \exp(-h\nu/\kappa T_x) \qquad (23)$$

with kT_x = 15 and 30 keV is incident normally ($\vartheta_0 = 0$) on a plane-parallel atmosphere is given in Figure 2. The spectrum of the radiation emergent at an angle of $\vartheta = 0$ is illustrated by the solid line, and that incident at an angle $\vartheta = \pi/2$ is illustrated by a dashed line. The corresponding values of the two-dimensional albedo are given in the lower part of Table I.

b. Reflection of X-Ray Radiation by the Surface of the Normal Component in a Binary System

It has been assumed in the numerical calculations that the normal component is a sphere of radius $R = 0.42 \cdot A$, where $A = 6 \cdot 10^{11}$ cm is the distance between the centers of the components (an analysis of the observational data for the system HZ Her results in such relations [6, 18, 7]). It has also been assumed that the x-ray source is a point and illuminates the entire portion of the normal star surface visible from it with x-ray radiation having a spectrum of the form $F_x(\nu) \propto \exp(-h\nu/\kappa T_x)$.

The x-ray brightness curves (the dependence of the radiation flux on observation phase $0 \leq \zeta \leq 1$, where $\zeta = 0$ corresponds to the middle of the x-ray eclipse) of the system HZ Her in reflected light are given in Figure 1b [the spectral $Q(\nu)$ for quanta with $h\nu$= 10, 20, and 30 keV] and in the upper part of Figure 1a [the integral $J = \int Q(\nu)d\nu$]. The temperature of the x-ray radiation of Her X1 has been assumed to be equal to kT_x = 30 keV. The integral brightness curve of the system is normalized to the primary flux of energy from Her X1 per unit solid angle $L_x/4\pi$, and the spectral $Q(\nu)$ have been normalized to the spectral flux of the primary x-ray radiation per unit solid angle at $h\nu \ll kT_x$. The x-ray brightness of the system in reflected light has been determined as the flux of the reflected radiation per unit solid angle in the direction of the observer from the

/14

entire visible part of the normal component. Also integral x-ray brightness curves of HZ Her in reflected light are given for comparison in Figure 1a for i = 0° and i = 15° along with the x-ray brightness curve of the source Cyg X3 (below).

In order to find the flux of reflected radiation at the Earth, it is sufficient to divide the value given in the figures by the square of the distance to the source r and take into consideration the normalization: $f_\nu(\nu) = Q(\nu, \zeta, i) \frac{h}{I_\nu} \frac{L_\nu}{4\pi r^2}$ (ergs/cm^2 sec Hz), $f_x = \int_0^\infty f_\nu(\nu) d\nu = J(\zeta, i) L_x / 4\pi r^2$ (ergs/cm^2 sec). On a change in the system parameters, the functions $Q(\nu, \zeta, i)$ and $J(\zeta, i)$ depend only on the ratio R/A [in the limit R/A $\ll$ 1, they are proportional to $(R/A)^2$]. In the case in which the normal star fills its Roche lobe, the ratio R/A depends weakly on the mass equation of the components M_x/M_v.

The spectrum of the reflected radiation is practically the same as that given in Figure 2. The maximum of the reflected flux occurs at $h\nu$ = 20 keV. A characteristic peculiarity of the curves given is the significant width of the eclipses in reflected light, exceeding by approximately a factor of three the width of the eclipses in the direct x-ray radiation of Her X1. The brightness curves in reflected x-ray radiation for kT_x = 15 keV have an analogous form.

IV. Effects Accompanying X-Ray Radiation Reflection

a. Spectral Peculiarities of the Reflected Signal

When $\nu \lesssim \nu_0$, an overwhelming portion of the emergent quanta experience only a single scattering, and the spectrum of the reflected radiation is completely determined in this case by the dependence of the photoabsorption cross section $\sigma_{pk}(\nu)$ on the

frequency. Because of this fact, there should appear in the reflected radiation spectrum absorption discontinuities corresponding to the boundaries of the K-series of the more abundant heavy elements O, Ne, S, Fe, etc. The average spectral index when $\nu \ll \nu_0$ is equal to $\alpha = 3$, i.e., the average spectrum of the reflected radiation in the case of the declining form of Equation (23) is similar to a Wien spectrum. The computed spectrum is given in Figure 2, and absorption discontinuities corresponding to sulfur and iron are displayed. The discontinuity corresponding to iron at $h\nu = 7.2$ keV is especially interesting, since it lies in the region of the spectrum in which the reflected radiation intensity is high. The ionization cross section at the threshold was taken equal to $\sigma_{Fe} = 4.6 \cdot 10^{-20}$ cm^2 in the estimates of the discontinuity magnitude, and the abundance of iron was assumed to be $[Fe]/[H] = 4 \cdot 10^{-5}$. It is difficult to caclulate for observation of a large number of the K_α-lines of the heavy elements, since for atoms with a relatively small nuclear charge Z (oxygen, neon, sulfur, and others), the probability of the Auger effect after the photo-removal of a K-electron significantly exceeds the probability of radiative decay and the emission of a K_α- quantum. The fluorescence probability ω_k increases in proportion to Z^4. Only the K_α-line of weakly ionized iron $h\nu = 6.5$ keV can appear intensely. For iron $\omega_k = 0.34$ [18a], i.e., 34% of the hard x-ray quanta absorbed upon the photoionization of iron should be reprocessed into K_α-quanta of iron. About one-half of them emerge from the photosphere without being absorbed. The natural line width is small, $h\Delta\nu \approx 10$ eV. It should be somewhat widened on the low frequency side, since part of the emergent quanta have experienced scattering and have lessened their frequency due to the recoil effect. The intensity of the K_α-line of iron in the reflected radiation depends (just as does the absorption discontinuity) only on the iron abundance in the star photosphere. With the abundance value

/15

adopted above, the intensity of this line is so greater that in narrow spectral integral $h\Delta\nu \lesssim 100$ eV, $\Delta\nu/\nu \sim 1/60$, its intensity should exceed the intensity of the primary signal in the same spectral integral. (This estimate takes into account the system geometry.) Consequently, this line may be detected in bright x-ray sources which are components of close binary pairs, /16 and its intensity should contain information about the iron abundance in the photospheres of normal stars. In particular, observation of the K_α-emission of iron in the spectrum of Sco X1 could serve as an additional criterion for its duplicity, the possibility of which is being discussed in the literature [22, 7]. We note that the intensity of this line should depend on the orbital inclination angle i.

b. High Temperature Scattering Layer above the Star Surface and Its Role in the X-Ray Radiation Reflection

The interaction of x-ray radiation with the normal star atmosphere induces a stellar wind, that is, it results in an effective evaporation and outflow of material from its surface [7, 9] (see Figure 6). The outflowing gas located in a field of hard radiation is heated up to high temperatures. The high degree of ionization of the elements determining the photoabsorption of x-ray photons results in a decrease in the role of photoabsorption processes in comparison with Thomson scattering. The optical thickness (for Thomson scattering) of this high temperature scattering layer lying above the star surface may be significant, $0 < \tau \lesssim 1$. Numerical calculation [7] has shown that, in the specific case of the HZ Her = Her X1 system, it amounts to $\tau_0 = 0.05$ (but it may be larger in other cases). Oxygen, carbon, helium, and hydrogen are completely ionized in this layer. The ratio of the concentration of OVIII and OIX ions amounts to only 10^{-2} — 10^{-3}. The optical thickness of the high temperature zone for photoabsorption appears

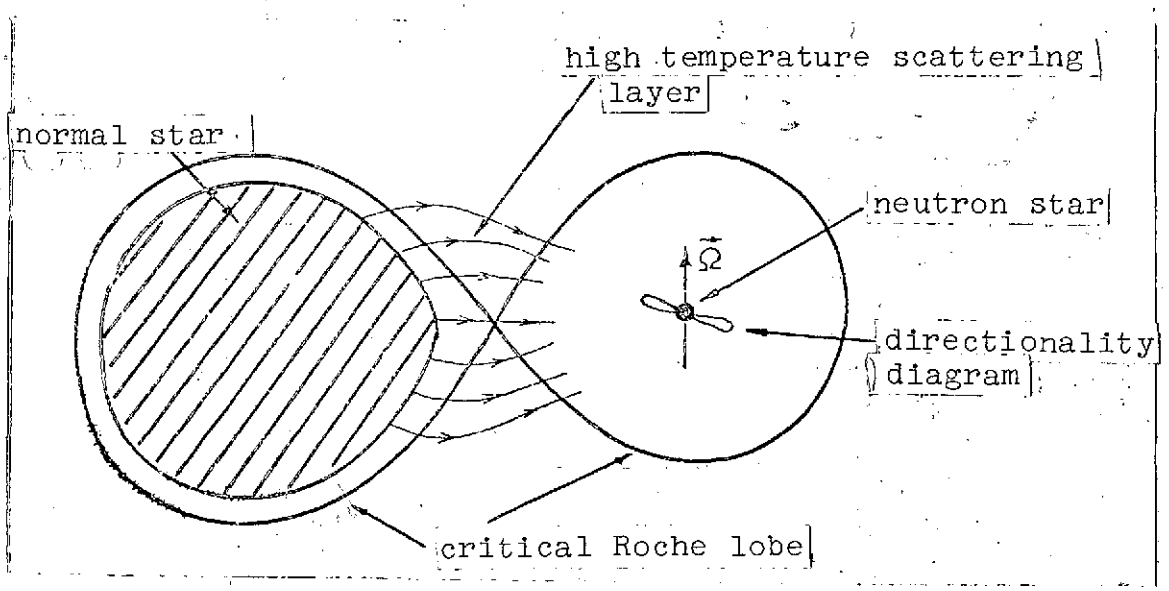

Figure 6. Binary system with x-ray pulsar and ionized reflecting layer arising upon the evaporation of material from the surface of the normal component.

to be small for all quanta with $h\nu \gtrsim 2$ keV. The supplementary contribution produced by this layer to the reflection of x-ray radiation results in a significant increase in the reflected flux in the $h\nu \sim 2$ — 10 keV region.

The effect of an external layer with optical thickness τ_0, in which pure scattering (the recoil effect can be neglected when $h\nu \lesssim 8$ keV) occurs, can easily be taken into account using /17 the well-known solution in planetary physics of the problem of the reflection of light by an atmosphere of finite thickness for a known albedo of the planet surface [16] (below, we will assume the surface albedo to be zero). It is possible to use, with sufficient accuracy, the approximate equations for the plane-parallel and spherical albedos

$$A_{sp} = \frac{\tau_0}{\tau_0 + 4/3}; \qquad A_p = \frac{3\tau_0 - (1 - e^{-\tau_0})}{4 + 3\tau_0}.$$

As a result, the spectrum of reflected x-ray radiation in the $h\nu \sim 2 - 20$ keV region may be flat and have the form illustrated by the dot-dashed line in Figure 2. The horizontal dashed lines on this same figure indicate the value of the reflected radiation intensity obtained in the limit $\nu \to 0$ in the presence of an external scattering layer in the plane-parallel atmosphere with a different optical thickness $\tau = \tau_0$. The characteristic value of the frequency ν_0 at which $\sigma_{ph}(\nu_0)\tau_0/\sigma_r \sim 1$ and the spectrum begins to be flat (the low frequency boundary of the spectrum) is determined by the degree of ionization of the heavy elements. This boundary may be variable and change in correspondence to variations in the intensity of the primary x-ray radiation or in the rate of acretion onto the compact components.

c. Polarization of the Reflected Radiation

Unpolarized radiation after scattering by electrons is linearly polarized, and the degree of polarization is $\mathcal{P}=1-\cos^2\gamma$, where γ is the scattering angle. Therefore, x-ray radiation reflected by the surface of the normal star should be linearly polarized. The reflected radiation with $h\nu \lesssim 8$ keV has experienced only a single scattering. The polarization of the emergent radiation in this case is easily estimated (the calculations for a plane-parallel atmosphere are cited in [26]). Due to the symmetry of the star surface at a phase of $\zeta = 0.5$, polarization of the reflected signal is absent. As the phase changes, the degree of polarization of the reflected signal rapidly increases, attaining a maximum of $\mathcal{P}\sim 60\text{-}80\%$ at $\zeta - \zeta_1 \sim 0.25$ and /18
$\zeta - \zeta_2 \sim 0.75$. The degree of polarization decreases for quanta with $h\nu > 8$ keV, since an appreciable contribution to the intensity of reflected radiation is made by quanta which have undergone several scatterings and, consequently, are weakly polarized. If the primary signal was polarized, then reflection

results in a noticeable depolarization and a change in the type of polarization. This effect is easily taken into account in each specific case in the approximation of a single scattering. Measurements of the linear polarization and its dependence on the observation phase can facilitate extraction of the reflected signal against the background of the primary signal.

d. Short Period Pulses of Reflected X-Ray Radiation

Pulsed x-ray radiation (with a period p of the order of several seconds) is incident on the surface of the normal component in the Her X1 = HZ Her system and in the binary system containing the x-ray source Cen X3. The pulses should be washed out on reflection. Their amplitude in the reflected x-ray radiation depends on two factors (below the star is assumed to be a sphere of radius R, and A is the size of the binary system):

1. the finite "wandering" time of x-ray quanta in the normal component atmosphere, td; and

2. the finite and the dimensions of the reflecting surface which are finite and comparable to pc: the reflected signal from various sections of this surface arrives at the observer at different phases of the x-ray pulses. Let us estimate the time t_d. The density distribution in the normal component atmosphere can be assumed with sufficient accuracy to be exponential, $Ne(z) = N_{e0} \exp(-z/H)$, where $H = (kTeR^2)/(m_p GM)$ is the thickness of a uniform atmosphere. We have $H \sim 10^8$ p cm for a star with the parameters of HZ Her. Introducing the Thomson scattering optical thickness $\tau = \int_z^\infty N_e(z) G_T dz$, we find $N_e(\tau) = \tau/G_T H$. The number of scatterings $\bar{N}_1(\nu)$ occurring, on the average, for each outward-bound photon is significantly less than $\bar{N}(\nu)$, which is cited in Table I and calculated per each incident photon. We note that /19

17% of the quanta emerge already after the first scattering, and quanta which have undergone many scatterings find themselves at great depths, lose energy as a result of the recoil effect, and are absorbed in the majority of cases. The stay time of an outward-bound photon in the atmosphere is

$$t_d(\nu) < \bar{N}_1(\nu)/\sigma_T N_e(\bar{\tau}) c \approx \bar{N}_1(\nu) H/\bar{\tau} c$$

Here $\bar{\tau} \gtrsim 1$ is the optical depth at which the majority of the scatterings take place. Most likely $\bar{\tau}$ is only a few times smaller than $\bar{N}_1(\nu)$, and $t_d(\nu) < 10(H/C) \approx 0.03$ sec $\ll 1.24$ sec. Thus, the delay time of the reflected x-ray photons on the normal star atmosphere is small, and the reflected flux pulse amplitude is determined by the finite dimensions of the reflecting surface.

It is not difficult to estimate the reflected x-ray flux pulse amplitude for an orbital inclination i = 90° at an observation phase $\zeta = 0.5$ (the maximum x-ray brightness in reflected light) in the limiting case of pulses infinitely narrow in time and isotropically emitted by a point source as

$$L_x(t) = 4\pi \mathcal{L}_x(t) = 4\pi \langle \mathcal{L}_x \rangle p \sum_{k=-\infty}^{k=+\infty} \delta(t - kp). \qquad (24)$$

Here p is the pulse period, and $\langle \mathcal{L}_x \rangle$ is the luminosity of the primary x-ray source per unit solid angle averaged over the pulse period. With such a form for the pulses, the observer will see a system of dispersing concentric bright rings on the normal star surface. The x-ray emission of each of these rings in the observer's direction rapidly falls off with their distance from the center — the point on the star surface nearest to the source of primary radiation (see Figure 7), and it is easily estimated. Therefore, the variability of the reflected signals is associated mainly with the rapid intermittent formation of a new ring and the slow decay of its intensity up to the instant of

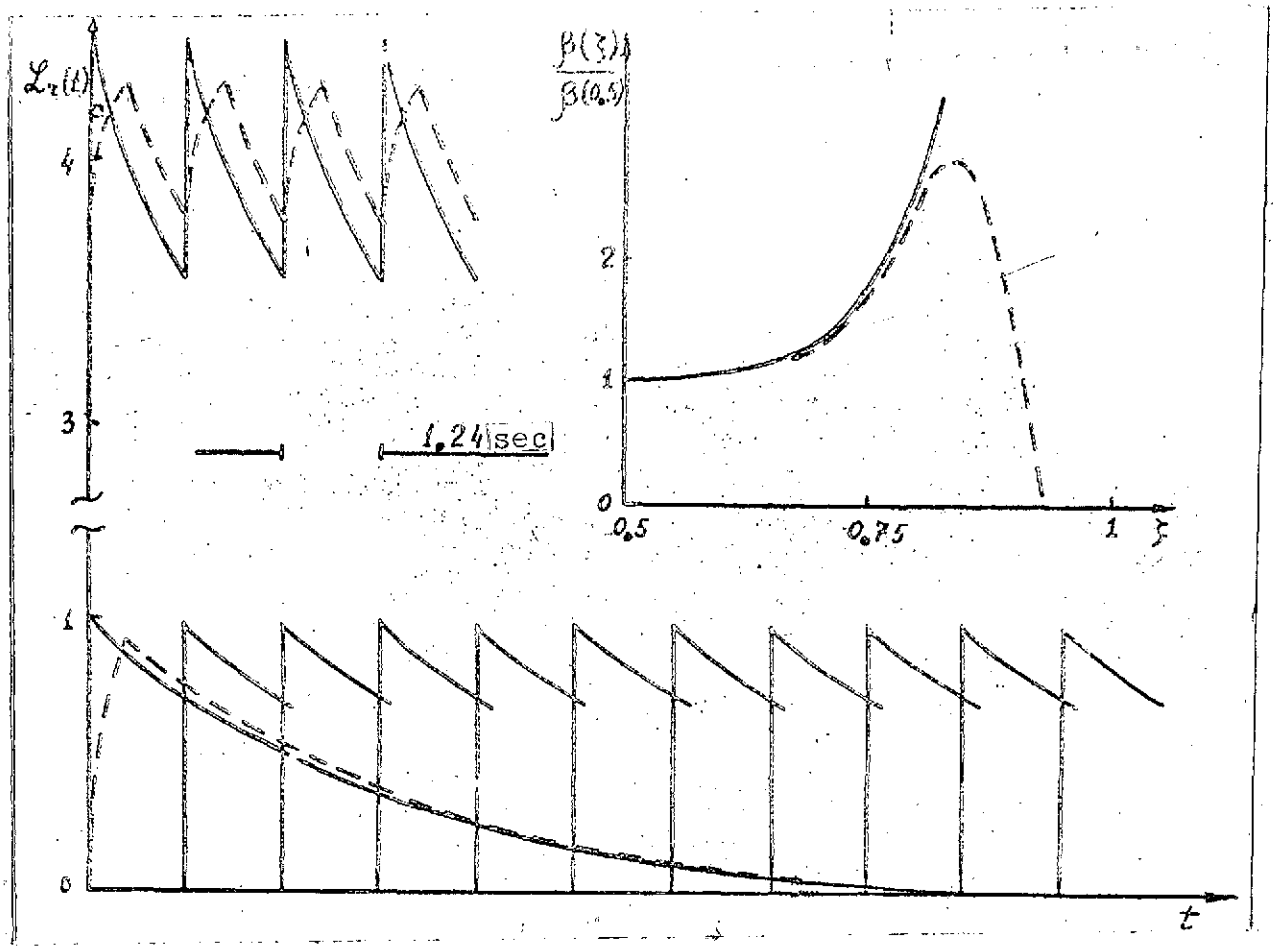

Figure 7. Pulses of the reflected x-ray signal in the system HZ Her. A plot of the luminosity of each ring-shaped band (see Section IVd), is given in the lower part of the figure, and the total flux from all bands to the observer is given in the upper part of the figure. The solid line corresponds to infinitely narrow pulses of the primary radiation (24), and the dashed curve corresponds to rectangular pulses with a duration of $\Delta p = p/3$. Such pulses should be observed in the case of a knife-edged directionality diagram. The dependence of the amplitude of the pulses of reflected x-ray flux (solid line) and optical pulses (dashed line) on the orbital phase is illustrated in the upper right-hand corner of the figure.

the next ring's origin. The total radiation of the remaining ($\left[L A \sqrt{A^2-R^2} - (A-R)^2\right]/cpA \approx 9.5$ in the case of HZ Her) rings provides /20 a slowly varying background. Assuming the delay time of quanta in the atmosphere to be $t_d = 0$, it is easy to find the size of

the discontinuity in the intensity of the reflected signal (per unit solid angle) upon the formation of a new ring, namely

$$\mathcal{L}_{r_0} = 2\rho(1,1)\frac{\langle \mathcal{L}_x \rangle}{\Lambda}\frac{R^2}{(A-R)(2A-R)}, \qquad (25)$$

where $\Lambda = R/cp$ and $\rho(\mu,\mu_0) = \int I(\nu,\tau,\mu,\mu_0)d\nu\big|_{\tau=0}$ is the reflection coefficient of a plane-parallel atmosphere (the x-ray flux reflected at an angle arc cos μ when the flux incident externally at an angle of arc cos μ is equal to $\pi\mu_0$). The determination of $I(\nu,\tau,\mu,\mu_0)$ is given at the start of Section III, and the values of $I(\nu,0,1,1)$ are given in Figure 2. The time-average intensity of the reflected signals (the mean sum for all the rings) is equal to

$$\mathcal{L}_r = 2\langle \mathcal{L}_x \rangle \int_{R/A}^{1} \rho(\mu,\eta)\frac{\eta\,\mu\,d\mu}{(A/R)^2+1-2A\mu/R}, \qquad (26)$$

where $\eta = (A\mu - R)/\sqrt{A^2+R^2-2AR\mu}$. The relative amplitude $\beta(s)\cdot\frac{\mathcal{L}_{r_0}}{\mathcal{L}_r}$ falls off inversely proportionally to $\Lambda = R/cp$ as the frequency of the primary x-ray radiation pulses increases. This quantity amounts to $\beta(s)_{s=0.5} = 0.3$ for the HZ Her system when $\Lambda = 6.7$. The amplitude of the reflected signal pulses is a minimum at the phase $s = 0.5$, i.e., at other phases $\beta(s) > 0.3$. This amplitude depends on the shape of the primary pulse, decreasing as its width increases. Using the solution derived for an incident signal of the form (24), it is possible in principle to derive by simple integration a solution for an arbitrary shape of the primary radiation pulses. In particular, one can show for rectangular pulses of duration Δp that the answer is close to $\beta(s)(1-\frac{\Delta p}{p})$. Observations of the pulsar Her X1 give $\Delta p \sim p/3$, and the pulse amplitude $(t_{max}-t_{min})p\,/\int f(t)dt$ should be only 20% of the value of the reflected signal.

The shape of the reflected pulses is illustrated in Figure 7 for the case where $\Delta p \sim p/3$ and the pulsar diagram is knife-shaped. It would appear, in this case (also in the case of a pencil diagram), that the observer should see how the pulsar's light waves run around the star hemisphere from one edge to the other. Actually, $\Lambda = \frac{\rho}{cp} \gg 1$, and, just as in the problem discussed above, the observer should see bright concentric ring-shaped bands dispersing over the star surface from a specific point (this point is close to the inner Lagrange point at an observation phase $\zeta = 0.5$ when $\Lambda \gg i$). The total path from the source to this point and from it to the observer is smaller than for any other point of the star surface. /21

e. Short Period Pulses of the Optical Radiation

The solution expounded above for the problem of the amplitude of reflected x-ray signal pulses can be applied to an analysis of the problem of the origin of the optical radiation pulses of HZ Her [19]. It was pointed out earlier in [7] that emission lines accompanying a high temperature gas are emitted from an optically thin region and are a rapid response to x-ray pulses. The radiation received in lines should pulse, but the amplitude of the pulses should be equal to 10 — 20%, just as the amplitude of the reflected x-ray radiation. The lines provide a small part of the intensity of the star optical radiation; therefore, the amplitude of the optical pulses is small (0.1 — 0.2%). The dependence of this amplitude on observation phase is given in Figure 7. The exit time of optical radiation created in the atmosphere after the reprocessing of the pulse emissions is large, $t_d \gg 1.24$ sec, for a major fraction of the optical radiation, as has been shown in [7]; therefore, it is possible that emission lines producing a negligible contribution to the total optical luminosity are the determining factor of the

optical pulses. Observations are possible, in principle, of the rapid variability in the optical emission lines of the bright optical objects which are the companions of the sources Cyg X1, 2U1700 — 37, and 2U0900 — 40. Irregular variability of the x-ray radiation has been detected in these sources with characteristic times ranging from 0.1 sec to 10 minutes. The intensity of the emission lines (He II highly ionized heavy elements, and /22
also the \Balmer\ lines) produced in the hot superphotospheric zone heated by x-ray radiation should vary in agreement with the temporal variations of the x-ray flux. Since the intensity of the lines depends strongly in a complicated manner on the plasma temperature, different types of correlation are possible. The thermal relaxation time in an optically thin zone is short, and the amplitude of variation of the radiation in the emission lines depends basically on the parameter $\Lambda = R/cp$. In the best cases in which the characteristic x-ray variation time is large $p \sim K/C$, this amplitude can be close to the amplitude of variation of the soft (0.5 — 10 keV) x-ray radiation. With $p \sim 0.1$ sec and $R \sim 10^{12}$ cm (the case of the source Cyg X1), the amplitude of the variation of the emission lines is only 0.1 — 1%. Optical emission lines associated with the reprocessing of x-ray radiation in the external regions of a disc composed of material \created\ by the relativistic object [4] and also by gas flows in the system can give a definite contribution to the optical variability of the systems.

Observations of the rapid optical variability in emission lines can clarify the mechanism for the reprocessing of x-ray radiation. We note that electron scattering makes a significant contribution to the opacity of hot stars. Therefore, a significant fraction of the x-ray radiation is absorbed in a zone which is optically thin to the emergent optical quanta. Consequently, the variable component of the optical radiation may be significant even in spite of the fact that the optical luminosity of

these systems significantly exceeds the x-ray luminosity.

V. Effects of Reprocessing and Reflection of X-Ray Radiation in Specific Systems

A. The Her X1 = HZ Her System

The value found for the two-dimensional albedo (Table I) permits drawing the conclusion that the region of the normal component surface nearest to the x-ray source reflects no more than 30 — 40% of the energy incident on it. The remaining 60 — 70% of the energy of the hard x-ray radiation is reprocessed into heat in the photospheric layers of the normal components and emerges in the form of optical and ultraviolet radiation with a Planckian spectrum. As a result, a bright hot spot is formed on the optical component surface with an effective temperature of $T_{eff} \approx T_0 \sqrt[4]{1+\beta_x F_x/F_0}$, where T_0 and F_e are the effective temperature and energy flux from the star interior in the absence of an irradiating x-ray flux, and $\beta_x \approx 0.6$ is the fraction of the energy absorbed. As has been shown in [7] and confirmed by the present calculations, the albedo of the observed hard x-ray radiation of Her X1 is completely sufficient to provide the observed optical variability of HZ Her. Since $F_x \gg F_0$, the maximum temperature of the photosphere is equal to $T_{eff} = \sqrt[4]{\beta_x F_x/\beta} = \sqrt[4]{\beta_x L_x/4\pi\beta A_1^2} \approx 2\times10^4$°K, i.e., upon adoption of the system parameters [7] of $L_x = 10^{37}$ ergs/sec and a distance from the x-ray source to the Lagrange point of $A_1 = 2.5\times10^{11}$ cm, it can even exceed the observed temperature. Here β is the Stefan-Boltzmann constant.

/23

a. 36-day periodicity of Her X1

Thus far, the nature of the variability of the x-ray source Her X1 with a 36-day period has not been explained: radiation

is observed at the Earth only during 12 days out of the 36. The optical variability of HZ Her with the system period being P = 1^d, which is associated with the reprocessing of the x-ray radiation of Her X1 in the normal component atmosphere, is observed during the entire 36-day cycle and does not disappear for 24 days [20]. Two alternatives exist:

1) the x-ray source precesses with a 36-day period [21 — 23] and illuminates the Earth 12 days out of 36; the normal star, which has enormous angular dimensions $\Omega \sim 0.6$ steradians when observed from the source, is illuminated to some extent or other constantly at 36 days; /24

2) hard x-ray radiation with $h\nu > 2$ keV is periodically switched on [24, 25], but there is constantly operating a source of soft x-ray radiation with $h\nu < 1$ keV, which heats up the hot spot on the surface of HZ Her and maintains the optical variability with the system period [13, 8]. A decisive argument in choosing between these two alternatives would be the observation of hard x-ray radiation with $h\nu \sim 15$ — 30 keV. In case 1), the intensity of the reflected (observable during 24 days of the 36) x-ray flux should amount to approximately 10% of the maximum level and vary with a period of P = $1^d.7$ (Figure 1). Pulses with a period of P = 1.24 sec in the reflected flux should be suppressed. Their amplitude should amount to approximately 10 — 20% of the reflected signal level. In case 2), the hard x-ray radiation should be absent during 24 days, the same as the softer x-ray radiation with $h\nu \sim 2$ — 6 keV.

We note that it is possible to hope for the extraction of a reflected signal for $h\nu > 6$ keV against the primary flux background. The strong (variable with the system period) polarization of the reflected radiation facilitates this extraction.

The small amplitude of the short-period pulses permits hoping for observations of the reflected signal between pulses of the primary radiation. The powerful K_α-line of iron may, in principle, be detected upon detailed spectral observations.

b. Possibility of the existence of a soft x-ray source in the system

The second possibility for explaining the 36-day cycle discussed in the preceding section suggests the presence in the HZ Her system of a soft x-ray source. It will be shown below that such a possibility is highly unlikely — the reprocessing of soft x-ray radiation in the normal star atmosphere cannot result in the optical phenomena observed in HZ Her.

We briefly recall these phenomena. UBV and spectral observation [6, 19, 26] show that the temperature of the surface on the star hemisphere which is turned toward the x-ray source drops off rapidly with distance from the point nearest the x-ray source. Absorption lines corresponding to the spectral classes B2 — A7 are observed [26]. This observation indicates that the optical radiation (formed as a result of the reprocessing of the energy of the x-ray flux) emerging from the star photosphere passes through layers lower in temperature than the radiation temperature, i.e., the x-ray radiation gets to a significant depth in the atmosphere. As was shown in [7], the reprocessing of the hard x-ray radiation of Her X1 explains the observed properties of HZ Her. Can a soft x-ray source of such power result in these properties? /25

The agreement of the spectral classes of HZ Her at different phases, which were determined independently according to UBV [6] and spectroscopic observations [19, 26], indicates

conditions close to local thermodynamic equilibrium at each point of this star photosphere. Therefore, the temperature in the region in which the optical spectrum is reprocessed cannot be greater than $T_e \lesssim 1.6 \cdot 10^{4\circ}$ K, which corresponds to the earliest spectral class observed for this star, namely, B2. At such a low temperature, the photoabsorption cross section of x-ray quanta having 55 eV < hν < 1 keV is great, which takes place primarily by He I and He II ions and also those of carbon and oxygen. Let us assume, in the atmosphere of HZ Her (M = 1.7 $M_\odot$, R = $2.5 \cdot 10^{11}$ cm) an exponential density distribution $N_e = N_{e0} \exp[-(z/H)]$, where $H \approx (kT_eR^2/m_pGM) \approx 2.3 \cdot 10^4 T_e \approx 5 \cdot 10^8$ cm. Then at a depth with an optical thickness based on free-free absorption (which gives the main contribution to the opacity at $T_e \sim 1.6 \cdot 10^{4\circ}$ K) of

$$\tau_{ff} = \int_0^\infty k_{ff}\, dz = 6.5 \cdot 10^{-24} N_{e0}^2 T_e^{-3/2} H/2 = 1 \qquad (27)$$

the optical thickness for photoabsorption is 80, even for quanta with hν = 1 keV and is $2.6 \cdot 10^3$ and $3 \cdot 10^5$ for quanta with hν = 250 eV and 50 eV, respectively. The free-free absorption coefficient has been taken here to be $k_{ff} = 6.5 \cdot 10^{-24} N_e^2 T_e^{-3.5}$ cm^{-1} [27]. The density $N_e \sim 7 \cdot 10^{14}$ cm^{-3} in the zone in which the emission spectrum is formed is easily estimated from condition (27). Recombination processes are effective at such a large density and low temperature, and the degree of ionization of the heavy elements and helium cannot be so high as to weaken the photoabsorption of x-ray quanta. Thus, soft x-ray radiation should be absorbed in a region optically thin for free-free processes and cannot be reprocessed into Planckian radiation. We recall that the optical thickness for photoabsorption is comparable to the optical thickness for free-free processes (in the model under discussion) for quanta with hν ~ 4 keV, but quanta with hν ~ 20 — 30 keV make the main contribution to the energy flux in the observed

/26

x-ray spectrum of Her X1. We assume the other possibility, namely, that the observed optical radiation is produced in a high temperature region of the atmosphere which is optically thin for pure absorption [9] to be highly unlikely (where then are the absorption lines formed?). In this case, the energy requirements on the model sharply increase: an optically thin hot plasma emits a small part of its energy in the optical region. A significant part of the intensity of the optical emission should be concentrated in emission lines, which is not observed.

B. X-Ray Pulsars into Whose Directionality Diagram the Earth Does Not Fall

The results of this article permit us to point out the possibility of the existence of a population of x-ray sources which radiate weakly in the well-studied spectral region $h\nu \sim 2 — 6$ keV and are bright at $h\nu \sim 15 — 20$ keV. These sources should be characterized by a sinusoidal variability in time with periods typical for close binary systems. We suggested that:

1) there exists a close binary system which includes a /27
a compact source of primary x-ray radiation and a normal star which fills its critical Roche lobe;

2) the narrow directional radiation of the primary source (a neutron star?) does not fall on the Earth, but due to the large angular dimensions of the normal component ($\Omega \sim 0.5 — 1$ steradians), part of its surface is continually illuminated by the x-ray flux.

There is nothing unusual about these suggestions; the x-ray pulsars Her X1 and Cen X3 are members of close binary systems and have rather narrow directional diagrams. There should exist

directions in which they do not radiate.

a. Spectrum of the reflected radiation

With a typical spectrum for the x-ray source $F_x(\nu) \propto \exp(-h\nu/kT_x)$ with $kT_x \sim 20$ — 40 keV, the spectrum of the reflected radiation is similar to a Wien spectrum with a maximum at $h\nu \sim 15$ — 20 keV. Subtle spectral effects associated with the K-jumps in the photoabsorption cross section and with the emission of K_α-quanta of iron, sulfur, and other elements are possible (see Figure 2 and Section IVa).

b. Variability

It is possible to receive, on the Earth, x-ray radiation reflected from the surface of the normal component. The rotation of the binary system results in a variability of the reflected x-ray flux with a period of the binary system and with an amplitude strongly dependent on the orbit inclination. The x-ray brightness curves in reflected light for a binary system with i = 90°, 15°, and 0° (straight line) are shown in the upper part of Figure 1a. The shape of these curves depends weakly on the specific parameters of the binary system if the normal component dimensions are close to the dimensions of the critical Roche lobe. For comparison, the x-ray brightness curve in direct rays is illustrated for the case of i = 90°.

c. The source Cyg X3

The curve in Figure 1a corresponding to i = 15° resembles the x-ray brightness curve of the source Cyg X3 [28], which has /28
not been explained up to now. It is possible that this source is a binary system of the type being discussed. (We note that

the small orbital inclination complicates the detection of the system optical variability.) Spectral peculiarities (the flat spectrum in the relatively soft $h\nu \sim 3 - 6$ keV x-ray region) of the source Cyg X3 could easily be explained by the presence in the system of an ionized scattering region with $\tau_0 \sim 0.3$ (see Section IVb). The reflected radiation should be linearly polarized at all observation phases, since the orbital inclination is small.

The primary pulses of the x-ray flux may be significantly weakened in the reflected signal. When the received signal is deflected mainly from the high-temperature scattering layer of large extent $l \gtrsim pc$, the rapid variability of the reflected signal should be additionally weakened in comparison with the estimates of Section IVc due to the finite transit time of the light through this zone. We recall that noticeable pulses with characteristic times $0.1 \lesssim p \lesssim 1$ sec have not been observed for this source [28].

No more than 30% of the incident energy in the 2 — 6 keV region can be reflected from the normal component surface. Since the luminosity of the primary source barely exceeds $L_x \approx 10^{38}$ ergs/sec, then adopting $kT_x \approx 30$ keV, it is easy to show that the system cannot be further away than 1.5 kpc in order to provide the observed x-ray flux. Based on the observations of absorption in the $\lambda 21$ cm line in the spectrum of a radio source which floats up near Cyg X3, the distance to it is estimated to be 8 — 11 kpc [29]. If these two peculiar objects, namely the radio source and the x-ray source, spatially coincide, the estimate cited for the distance offers great difficulty to the suggested interpretation of the x-ray brightness curve of Cyg X3.

The authors are greatful to Ya. B. Zel'dovich, I. L. Beygman, and A. M. Urnov for discussions.

REFERENCES

1. Tananbaum, H. Proceedings of IAU Symposium No. 55. R. Giacconi and H. Bradt, eds. Dordrecht, Reidel, 1972.

2. Gursky, H. Preprint, "Galactic X-Ray Sources." Lectures in Les Hourches, 1972.

3. Shklovskiy, I. S. Astron. zh., Vol. 44, 1967, p. 930.

4. Shakura, N. I., and R. A. Sunyayev. Astron. and Astrophys. Vol. 24, 1973, p. 317.

5. Bahcall, J. N., and N. A. Bahcall. Astrophys. J., Vol. 178, 1972, p. L1.

6. Lyutyy, V. M., R. A. Syunyaev, and A. M. Cherepashchuk, Astron. zh., Vol. 50, 1973, p. 3.

7. Vasko, M. M., and R. A. Sunyayev. Astrophys. and Sp. Sci. (in press), Preprint No. 8, Institute of Applied Mathematics, 1973.

8. Pringle, J. E. Preprint, 1973.

9. Arons, J. Preprint, 1973.

10. Bethe, H. A. and E. E. Salpeter. Quantum Mechanics of One- and Two-Electron Atoms. New York, Academic Press, 1957.

11. Brown, R. L. and R. J. Gould. Phys. Rev. D., Vol. 1, 1970, p. 2252.

12. Ulmer, M. P., W. A. Baity, W. A. Wheaton, and L. E. Peterson. Astrophys. J., Vol. 178, 1972, p. L61.

13. Avni, Y., J. N. Bahcall, P. C. Joss, N. A. Bahcall, F. K. Lamb, C. J. Pethick, and D. Pines. Preprint, 1973.

14. Bell, K. L. and A. E. Kingston. Mon. No. Roy. Astron. Soc., Vol. 136, 1967, p. 241.

15. Ivanov, V. V. Perenos izlucheniya i spektry nebesnykh tel (Radiation Transfer and the Spectra of Celestial Objects), Moscow, Nauka Press, 1969.

16. Sobolev, V. V. Rasseyaniye sveta v atmosferakh planet (Light Scatterings in Planetary Atmospheres). Moscow, Nauka Press, 1972.

17. Akhiezer, A. I., and V. B. Berestetskiy. Kvaitovaya elektrodinamika (Quantum Electrodynamics). Third Edition. Moscow, Nauka Press, 1969.

18. Forman, W., C. A. Jones, and W. Liller. Astrphys. J., Vol. 177, 1972, p. L103.

18a. Fink, R. W., R. C. Jopson, Mark Hans, and C. D. Swift. Rev. Mod. Phys., Vol. 38, 1966, p. 513.

19. Davidson, A., J. P. Henry, J. Middleditch, and M. E. Smith. /30 Astrophys. J., Vol. 177, 1972, p. L97.

20. Wenzel, W. and M. Hessner. IBVS, No. 733, 1972.

21. Brecher, K. Nature, Vol. 239, 1972, p. 325.

22. Shklovskiy, I. S. Astron. zh., Vol. 50, 1973, p. 233.

23. Novikov, I. D. Preprint of the Institute of Applied Mathematics, 1973.

24. Tanabaum, H., H. Gursky, E. M. Kellogg, R. Levinson, E. Schreier, and R. Giacconi. Astrophys. J., Vol. 174, 1972, p. L143.

25. Bisnovatyy-Kogan, G. S., and B. V. Komberg. Preprint of the Institute of Applied Mathematics, 1973.

26. Crampton, D., and J. B. Hutchings. Astrophys. J., Vol. 178, 1972, p. L-65.

27. Zel'dovich, Ya. B., and Yu. P. Rayzer. Fizika udarnykh voln i vysokotemperaturnykh gidrodinamicheskikh yavleniy (The Physics of Soft Waves and High Temperature Hydrodynamic Phenomena). Second Edition. Moscow, Nauka Press, 1966.

28. Parsignault, D. R., H. Gursky, F. M. Kellogg, T. Matilsky, S. Murray, E. Schreier, H. Tanabaum, R. Giacconi, and A. C. Brinkman. Nature, Vol. 239, 1972, p. 123.

29. Lauque, R., J. Lequeux, and Nguyan-Quang-Rieu. Nature, Vol. 239, 1972, p. 119.

Translated for National Aeronautics and Space Administration under contract No. NASw-2483 by SCITRAN, P. O. Box 5456, Santa Barbara, California 93108.